

# Molecular Dynamic Simulation on the Structure of Sodium Germanate Melts

Tokuro NANBA, Masahiro NAKAMURA and Yoshinari MIURA

Department of Environmental Chemistry and Materials, Okayama University, 3-1-1, Tsushima-Naka, Okayama 700-8530, Japan

**A molecular dynamic simulation with 2 + 3 body interactions was performed to investigate the structural changes in the sodium germanate melts. It has been widely accepted that the octahedral  $\text{GeO}_6$  units change into tetrahedral  $\text{GeO}_4$  units and non-bridging oxygen is formed while the glass is melting. Such the structural changes were confirmed in the simulations. Furthermore, oxygen atoms surrounded by three Ge atoms were also formed in the structural models, and the relative amount of the 3-fold oxygen decreased during the heating simulations. From these results, the glassy and molten states could be characterized by the edge-sharing connections by  $\text{GeO}_6$  units and the corner-sharing open structures by  $\text{GeO}_4$  units, respectively.**

[Received August 8, 2003; Accepted December 11, 2003]

**Key-words :** MD simulation, Structure, Germanate, Melt, Glass

## 1. Introduction

Glass has been regarded as a frozen-in undercooled liquid,<sup>1)</sup> and hence it has been commonly accepted that the structure of a glass is analogous to that of its melt. However, structural differences between glass and melt have been confirmed in various glass systems.<sup>1)</sup> For example, the dissociation of Si-O-Si bridges was found in silicate melts,<sup>2)</sup> and the change in coordination number of boron was observed in sodium borate system.<sup>3)</sup> As for alkali germanate system, the density measurements by Riebling<sup>4)</sup> and Sekiya et al.<sup>5)</sup> suggested that 6-fold coordinated Ge, Ge(6) were also present in the melts other than 4-fold coordinated Ge, Ge(4). By using X-ray radial distribution analysis, Kamiya et al.<sup>6)</sup> revealed that the atomic distance of the nearest Ge-Ge pairs was longer at higher temperatures while there was no great difference in the Ge-O distance. Based on Raman spectra, Yano<sup>7)</sup> indicated that non-bridging oxygen (NBO) was formed and the relative amount of  $\text{GeO}_4$  unit containing NBO increased in the melts. According to the radial distribution analysis,<sup>6)</sup> the decrease in the average Ge coordination number was confirmed and it was however not more than 5%, which seems to be quite small as compared with the change revealed in Raman spectra.<sup>7)</sup>

Molecular dynamic (MD) simulation is probably the most suitable method to investigate the structural changes in phase transition. The authors<sup>8)</sup> have applied MD simulation to the structural investigation of germanate glass, where the changes in the coordination structure were thoroughly examined both in heating and cooling processes. In the heat treatment simulation for the Ge(6)-containing rutile- $\text{GeO}_2$  and  $\text{Na}_4\text{Ge}_9\text{O}_{20}$  crystals, a sequential conversion in the coordination number of Ge, 6→5→4 was commonly observed at around the respective melting temperatures, where steep drops in density were also confirmed. The structural changes in the glass formation process, that is, the cooling process have been explored in the previous study,<sup>8)</sup> and hence in the present paper, the structural changes in the coordination structure and the formation of NBO during the melting stage were studied in detail by using MD simulation.

## 2. Computational procedures

The potential function used here consists of a Born-Mayer-Huggins (BMH) two-body interaction and a three-body interaction given by Anderson et al.<sup>9)</sup>

2-body term:

$$\left\{ \begin{aligned} \phi_{ij} &= \frac{z_i z_j e^2}{4\pi\epsilon_0 r_{ij}} B_{ij}(r_{ij}) \\ B_{ij}(r_{ij}) &= A_{ij} \left( 1 + \frac{z_i}{n_i} + \frac{z_j}{n_j} \right) \exp \{ (\sigma_i + \sigma_j - r_{ij}) \rho_{ij} \} \end{aligned} \right.$$

3-body term:

$$\left\{ \begin{aligned} \phi_{ijk} &= (\phi_{ij} + \phi_{ik}) \exp \{ -\gamma_{ijk} (\bar{\theta} - \theta_{ijk})^2 \} \\ \phi_{ij} &= -C_{ij} B_{ij}(\zeta_{ij}) \exp \{ (\zeta_{ij} - r_{ij}) \eta_{ij} \} \end{aligned} \right. \quad (2)$$

where  $z_i$  is the valence of the  $i$ -th ion,  $e^2/4\pi\epsilon_0$  is a constant ( $230.7 \times 10^{-30}$  Jm),  $r_{ij}$  is the inter-atomic distance,  $A_{ij}$  is an empirical constant,  $n_i$  is the number of electrons in the outer shell,  $\sigma_i$  is the size parameter,  $\rho_{ij}$  is the softness parameter,  $\theta_{ijk}$  is the bond angle,  $C_{ij}$ ,  $\zeta_{ij}$ ,  $\eta_{ij}$ ,  $\gamma_{ijk}$  and  $\bar{\theta}$  are empirical constants. The 3-body potential was applied to the structural units, O-Ge-O and Ge-O-Ge, in which the distances  $r_{\text{GeO}}$  were less than or equal to the cut-off distance,  $r_c$ . Structural models with the chemical compositions,  $x=0, 0.1, 0.2, 0.3$  and  $0.4$  in  $x\text{Na}_2\text{O} \cdot (1-x)\text{GeO}_2$  (molar ratio) were produced in the present study. The same parameter set<sup>8)</sup> was used in the MD calculations, except for the charge of oxide ion, which was adjusted for electro-neutrality. More detailed computational procedures have been reported elsewhere.<sup>8)</sup>

Firstly, glass models at room temperature (RT) were produced as follows. Total number of particles ( $N$ ) placed in an MD cell was 1023 at  $x=0$  and 1020 at  $x=0.1, 0.2, 0.3$  and  $0.4$ , and the particles were randomly arranged in a cubic box of volume  $V$ . After the relaxation at  $T=6000$  K for  $t=10$  ps under a constant-volume condition (NVT ensemble), the system was cooled stepwise every 100 K from 6000 K to 1300 K and every 50 K below 1300 K under a constant-pressure condition (NPT ensemble,  $P=0$  Pa,  $t=10$  ps) to obtain the glass model at RT. After an additional 40 ps NPT relaxation ( $T=300$  K,  $P=0$  Pa), a 4 ps NVT MD run was performed to compute vibrational spectra and radial distribution functions (RDFs). Next the glass models at RT were heated up inversely to obtain the melt models at higher temperatures. The melting point of sodium germanates is 1200–1400 K, and hence the MD models at  $T=1400$  K were examined in detail to evaluate the structure of melts. As shown in the previous paper,<sup>8)</sup> the cut-off distance,  $r_c$  has an influence not only on the coordination number of Ge but also on the density and melting temperature of a system. In the present study, therefore, the optimum  $r_c$  was explored to attain the appropriate density of the MD models in the cooling and heating simulations.

### 3. Results and discussion

#### 3.1 Comparison between simulation and experiment

Pair distribution functions  $g(r)$  were calculated from the MD models, and they were compared with the experimental ones to evaluate the validity of the simulations, where experimental data were collected from literatures.<sup>6,10-13</sup> As shown in **Fig. 1**, the  $g(r)$ s for the MD models with small  $\text{Na}_2\text{O}$  content are in good agreement with those of the glasses at RT, and at high  $\text{Na}_2\text{O}$  content, however, small disagreements are observed particular in the peak positions; at  $x=0.4$  the discrepancy in the first Ge-O peaks is 0.01 nm. As compared with the glassy state at RT, the disagreement in  $g(r)$  is insignificant at higher temperatures; while the discrepancy in the peak position is observed, the spectral characteristics are successfully reproduced. The discrepancy in the Ge-O bond length is due to the shorter distance in Ge-NBO bonds in the MD models.

Raman spectra were also simulated by Fourier transforma-

tion of a time correlation function  $\langle F_C(t) \cdot F_C(0) \rangle$ , where  $F_C(t)$  is given by  $\dot{\mathbf{r}}_i(t) \sum_j \mathbf{r}_{ij}(t) / |\mathbf{r}_{ij}(t)|$ ,  $\dot{\mathbf{r}}_i$  is the velocity vector of the particle  $i$ , and  $\mathbf{r}_{ij}$  is the vector pointing from the central particle  $i$  to the ligand  $j$  in a structural unit formed by the  $i$ - $j$  bonds.<sup>14</sup> Raman spectra of the structural units of  $\text{GeO}_n$  ( $i=\text{Ge}$ ,  $j=\text{O}$ ) and  $\text{OGe}_n$  ( $i=\text{O}$ ,  $j=\text{Ge}$ ) were calculated in the present study. As shown in **Fig. 2**,  $\text{GeO}_n$  units in the MD models give complicated Raman bands below  $700 \text{ cm}^{-1}$ , and the Raman bands of  $\text{OGe}_n$  units appear at  $700$ ,  $900$  and  $1100 \text{ cm}^{-1}$ . It has been commonly assigned that  $400$ – $700 \text{ cm}^{-1}$  bands are the bridging Ge-O-Ge vibrations and  $800$ – $900 \text{ cm}^{-1}$  bands are the non-bridging Ge-NBO vibrations.<sup>15,16</sup> According to the detailed analysis,<sup>8</sup> the  $700$ ,  $900$  and  $1100 \text{ cm}^{-1}$  bands in the calculated spectra are associated with  $\text{OGe}_3$ ,  $\text{OGe}_2$  and  $\text{OGe}_1$  units, respectively. The NBO ( $\text{OGe}_1$ ) band of the MD models appears at higher frequency region than that of the actual glasses. It is due to the disagreement in the atomic distance of Ge-NBO bond. The relative intensity of the

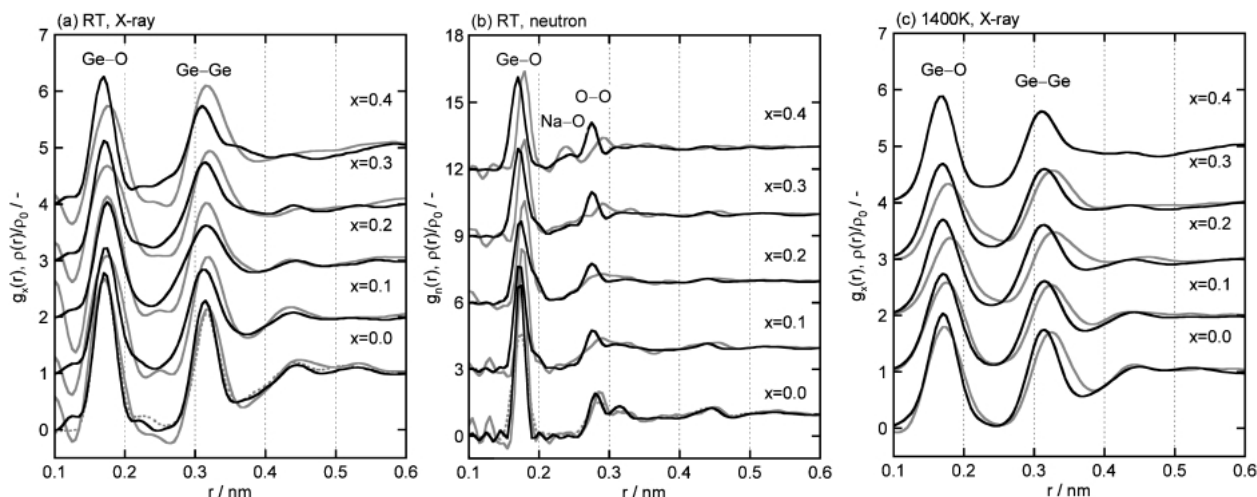


Fig. 1. Pair distribution functions, X-ray-weighted  $g_x(r)$  and neutron-weighted  $g_n(r)$ . The black lines are obtained from the 4 ps MD simulations at RT (300 K) and 1400 K for  $x\text{Na}_2\text{O} \cdot (1-x)\text{GeO}_2$ . The experimental  $g(r)$ s shown by the gray lines are cited from literatures; (a)  $g_x(r)$  for the glasses at RT from Refs. 10 and 11, (b)  $g_n(r)$  for the glasses at RT from Refs. 12 and 13, and (c)  $g_x(r)$  for the melts at 1373 K from Ref. 6.

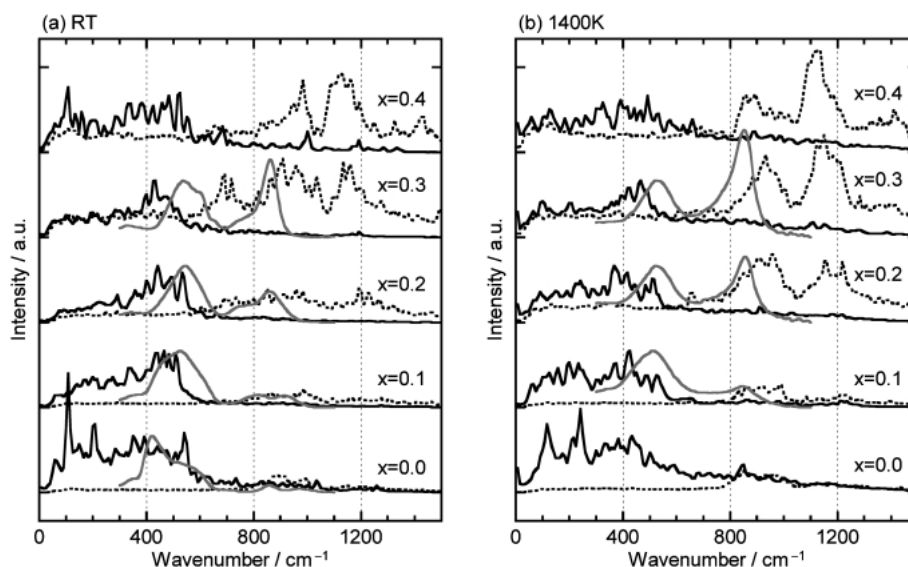


Fig. 2. Raman spectra simulated from the 4 ps MD runs at RT (300 K) and 1400 K for  $\text{GeO}_n$  polyhedra (solid lines) and  $\text{OGe}_n$  units (dotted lines) in  $x\text{Na}_2\text{O} \cdot (1-x)\text{GeO}_2$ . The experimental ones at RT and 1273 K (gray lines) are cited from Ref. 7.

NBO band is, however, in good agreement between the simulations and the experiments. With increasing  $\text{Na}_2\text{O}$  content, the NBO band ( $1100\text{ cm}^{-1}$ ) in the calculated spectra increases in intensity as compared with the BO ( $\text{OGe}_2$ ) band ( $900\text{ cm}^{-1}$ ).

The change in the coordination numbers of Ge and O during the heating simulations is shown in Fig. 3. The coordination number of Ge,  $C(\text{Ge})$  in every composition decreases with increasing temperature, which has been commonly interpreted as the conversion of  $\text{Ge}(6)$  into  $\text{Ge}(4)$ . The coordination number of O,  $C(\text{O})$  also decreases with increasing temperature, being interpreted as the conversion of BO into NBO. In the temperature region just below the melting points (1200–1400 K), the large drops both in  $C(\text{Ge})$  and  $C(\text{O})$  appear for the  $\text{Na}_2\text{O}$ -containing models. At around 1400 K,  $C(\text{Ge})$  shows a narrow distribution (3.9–4.1) as compared with  $C(\text{O})$  (1.5–2.0). In Fig. 3, the coordination numbers experimentally obtained<sup>(6),12)</sup> are also plotted by the gray markers. The values of  $C(\text{Ge})$  at 1373 K given in Ref. 6 seem to be larger than the actual values, and hence the experimental RDFs given in Ref. 6 are re-examined by the pair-function method.<sup>(17)</sup> As shown in Fig. 3(a), the difference in  $C(\text{Ge})$  at around 1400 K is small, except for the melt at  $x=0.3$ .

The disagreements are recognized between the simulations and experiments particularly in the higher  $\text{Na}_2\text{O}$  content,

which are responsible for the discrepancy in Ge–O bond length. It is necessary to improve the potential parameters to obtain the better agreements. However, the spectral features observed in the pair distribution functions (Fig. 1) and Raman spectra (Fig. 2) seem to be successfully reproduced by the present MD models. It is consequently judged that the MD models obtained in the present study are valid for the discussion in the structural changes during the melting process.

### 3.2 Structural change during melting process

As shown in Fig. 3, the coordination numbers of Ge and O in the MD models decrease during the heating simulations, suggesting the structural conversions of  $\text{Ge}(6)$  into  $\text{Ge}(4)$  and BO into NBO, that is, the dissociation of Ge–O–Ge networks. There seems to be no contradiction between the present simulations and the experiments.<sup>(4)–7)</sup> Is there anything left unnoticed in the experimental observations? Then, the structural changes during the heating simulations are examined in detail. The changes in the relative amount of  $n$ -fold coordinated Ge ( $n$ ) and O ( $n$ ) at  $x=0.2$  are plotted in Fig. 4. As shown in Fig. 4(a), 5-fold coordinated Ge,  $\text{Ge}(5)$  is present in the MD model, and the amount of  $\text{Ge}(5)$  is larger than that of  $\text{Ge}(6)$ . As concluded in the previous paper,<sup>(8)</sup> no significant improvements in RDFs or vibrational spectra have been observed even in the MD models not-containing  $\text{Ge}(5)$ , and the experimental evidence showing that  $\text{Ge}(5)$  is not present in germanate

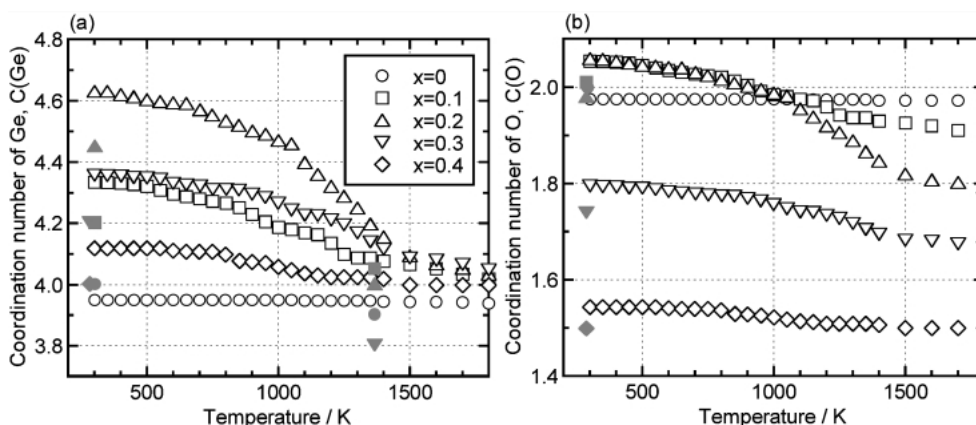


Fig. 3. Changes in the coordination numbers of Ge,  $C(\text{Ge})$  and O,  $C(\text{O})$  during the heating MD simulations for  $x\text{Na}_2\text{O} \cdot (1-x)\text{GeO}_2$ . The data shown by the open markers are the time average during the 10 ps MD runs. The gray markers indicate the experimentally obtained coordination numbers at RT from Ref. 12 and at 1373 K from Ref. 6.

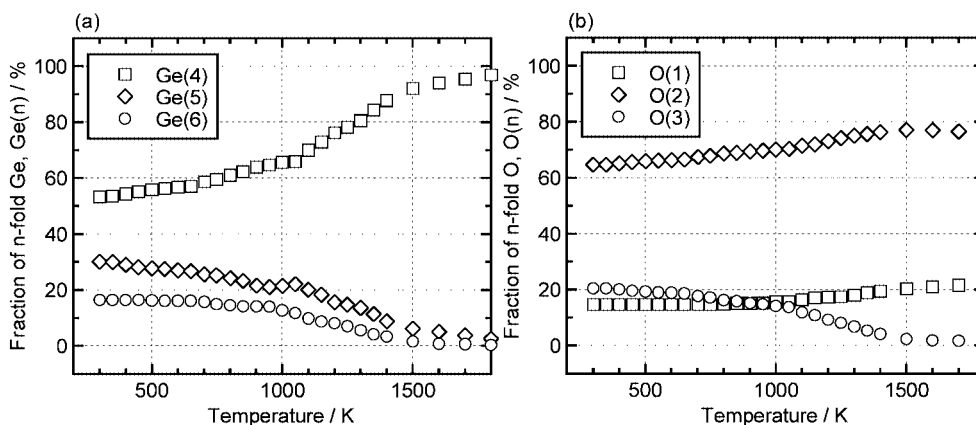


Fig. 4. Changes in the fraction of  $n$ -fold coordinated  $\text{Ge}(n)$  and  $\text{O}(n)$  during the heating MD simulations for  $0.2\text{Na}_2\text{O} \cdot 0.8\text{GeO}_2$ . The data shown by the markers are the time average during the 10 ps MD runs.

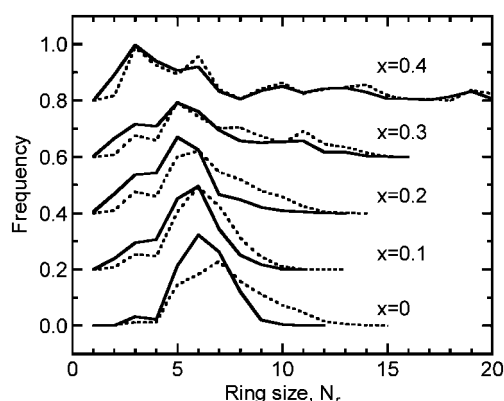


Fig. 5. Ring size distribution during the 4 ps MD runs at RT (continuous lines) and 1400 K (broken lines) for  $x\text{Na}_2\text{O} \cdot (1-x)\text{GeO}_2$ . The ring size  $N_r$  is the number of Ge atoms in a ring.  $N_r = 1$  and 2 indicate connections sharing a face and sharing an edge, respectively.

glasses or melts has not been given. In the temperature range between RT and 700 K, the fraction of Ge(6) is almost constant at 16% and the fraction of Ge(5) decreases with increasing the temperature. It indicates that the change in the coordination structure of Ge which takes place at the beginning is not the conversion of Ge(6) into Ge(5) but the conversion of Ge(5) into Ge(4), suggesting that Ge(5) possesses higher energy than Ge(4) and Ge(6). It is hence supposed that Ge(5) is transient species during the conversion between Ge(4) and Ge(6). If the MD model at RT were produced at much slower cooling rate, the amount of Ge(5) would be less than that of Ge(6). In any event, the amount of Ge(4) is ca. 90% at around 1400 K, indicating that Ge(5) or Ge(6) with higher coordination numbers decreases in content with increasing temperature but the amount of these species is not negligible in the melts.

As shown in Fig. 3(b), the coordination number of O decreases with increasing the temperature, from which it is expected that the NBO fraction increases and the BO fraction decreases during the heating simulations. As shown in Fig. 4(b), however, even BO designated as O(2) increases in fraction as contrary to the expectation. In the MD models, O(3) which is surrounded by three Ge atoms exists and the fraction of O(3) decreases with increasing the temperature. O(3) gives rise to edge-sharing  $\text{GeO}_n$  units with higher coordination numbers ( $n = 5$  or  $6$ ). The ring size distribution is plotted in Fig. 5, where the ring size  $N_r$  is the number of Ge atoms in a ring. With increasing  $\text{Na}_2\text{O}$  content, the distribution becomes broad and the most frequent size shifts from 6 to 3, indicating the increase in the edge-sharing connections. Comparing the distribution between RT and 1400 K, the small rings decrease and the large rings increase in the melts, indicating the conversion from the dense structure due to the edge-sharing connections to the open structure formed by the corner-sharing connections. It has been commonly accepted that the structural changes along with melting are the decrease in the Ge coordi-

nation number from 6 to 4 and the formation of NBO as the result of the network dissociation. It is also found in the present simulations that the conversion of Ge(6) into Ge(4) is accompanied by the change in the network connectivity from edge-sharing to corner-sharing, resulting in the open structures.

#### 4. Conclusion

The structural changes of sodium germanate glasses during the melting process were examined by using the molecular dynamic simulations. It has been generally accepted that the octahedral  $\text{GeO}_6$  units convert into tetrahedral  $\text{GeO}_4$  units and the dissociation of Ge-O-Ge bridges occurs to form NBO in the molten state. Such the structural changes were successfully reproduced in the MD simulations. Furthermore, some structural characteristics not proposed from the experimental observations were confirmed in the MD models. As for the glassy state, the structural units in higher coordination numbers,  $\text{GeO}_5$  and  $\text{GeO}_6$  prefer the edge-sharing connections through 3-fold coordinated O(3) rather than the corner-sharing ones via 2-fold O(2), namely BO. As for the molten state,  $\text{GeO}_5$  and  $\text{GeO}_6$  units turn into  $\text{GeO}_4$  units, and at the same time the edge-sharing to corner-sharing transition takes place, resulting in a open structure with lower densities.

#### References

- 1) Scholze, H., "Glass—Nature, Structure, and Properties," Springer-Verlag (1991) pp. 3–42.
- 2) Seifert, F. A., Mysen, B. O. and Virgo, D., *Geochim. Cosmochim. Acta*, Vol. 45, pp. 1879–1884 (1981).
- 3) Titov, A. P., Golubkov, V. V. and Porai-Koshits, E. A., *Sov. J. Glass Phys. Chem.*, Vol. 7, pp. 371–378 (1981).
- 4) Riebling, E. F., *J. Chem. Phys.*, Vol. 39(11), pp. 3022–3030 (1963).
- 5) Sekiya, K., Morinaga, K. and Yanagase, T., *J. Ceram. Soc. Japan (Yogyo-Kyokai-Shi)*, Vol. 88(7), pp. 367–372 (1980) [in Japanese].
- 6) Kamiya, K., Yoko, T., Itoh, Y. and Sakka, S., *J. Non-Cryst. Solids*, Vol. 79, pp. 285–294 (1986).
- 7) Yano, T., *NEW GLASS*, Vol. 17(1), pp. 20–26 (2002) [in Japanese].
- 8) Nanba, T., Kieffer, J. and Miura, Y., *J. Non-Cryst. Solids*, Vol. 277, pp. 188–206 (2000).
- 9) Anderson, D. C., Kieffer, J. and Klarsfeld, S., *J. Chem. Phys.*, Vol. 98, pp. 8978–8986 (1993).
- 10) Kamiya, K. and Sakka, S., *Phys. Chem. Glasses*, Vol. 20, pp. 60–64 (1979).
- 11) Leadbetter, A. J. and Wright, A. C., *J. Non-Cryst. Solids*, Vol. 7, pp. 37–52 (1972).
- 12) Ueno, M., Misawa, M. and Suzuki, K., *Physica*, Vol. 120B, pp. 347–351 (1983).
- 13) Erwin Desa, J. A., Wright, A. C. and Sinclair, R. N., *J. Non-Cryst. Solids*, Vol. 99, pp. 276–288 (1988).
- 14) Brawer, S., *J. Chem. Phys.*, Vol. 79, pp. 4539–4544 (1983).
- 15) Verweij, H. and Buster, J. H. J. M., *J. Non-Cryst. Solids*, Vol. 34, pp. 81–99 (1979).
- 16) Mochida, N., Sakai, K. and Kikuchi, K., *J. Ceram. Soc. Japan (Yogyo-Kyokai-Shi)*, Vol. 92, pp. 164–172 (1984).
- 17) Warren, B. E., "X-ray Diffraction," Dover Publications, Inc. (1990) pp. 135–142.